Available online at www.sciencedirect.com
SCIENCE DIRECT®
Applied Surface Science 222 (2004) 357–364
applied surface science
www.elsevier.com/locate/apsusc

Temperature effects on the growth of oxide islands on Cu(1 1 0)

Guangwen Zhou*, Judith C. Yang

Department of Materials Science and Engineering, University of Pittsburgh, 848 Benedum Hall, Pittsburgh, PA 15261, USA

Received 5 July 2003; received in revised form 3 September 2003; accepted 3 September 2003

Abstract

We examined the Cu_2O island formation on Cu(1 1 0) as a function of oxidation temperature in the range of 450–650 °C and oxygen pressure of 0.1 Torr. Epitaxial three-dimensional trapezoid island formation was observed for oxidation at the all temperatures and it was found that increasing oxidation temperature increased the thickening rate of the oxide islands. The oxidation at 0.1 Torr was noted to have a smaller nucleation activation energy for the oxide formation as compared to lower pressures.

PACS: 61.16.13g; 68.35.−a; 81.05.Bx; 81.65.Mq

Keywords: Oxidation; Cu(1 1 0); Cu_2O; Morphology; In situ ultra-high vacuum transmission electron microscope (UHV-TEM)

1. Introduction

A complete understanding of oxidation processes includes the investigation of the initial stages of oxidation, i.e., the nucleation and initial growth of the oxides which occur in the nanometer-size regime. The initial state of a metal surface, such as surface impurities and surface morphology, may greatly influence the oxide nucleation, growth and hence the oxide film structure [1]. The improved experimental techniques in ultra-high vacuum (UHV) now make it feasible to investigate surfaces that are atomically clean at the starting of the experiments, which is extremely important for quantitative understanding of oxidation kinetics. We are presently using a novel technique, in situ UHV-transmission electron microscopy (TEM), which combines the correct range in spatial resolution and provides the UHV environment necessary to control surface conditions.

Cu is considered to be a model system for the oxidation of metal for the fundamental understanding of oxidation mechanisms and has been studied extensively [2–4]. We had previously reported our investigations of the kinetics of Cu(1 0 0) and Cu(1 1 0) oxidation using in situ UHV-TEM, and demonstrated that oxygen surface diffusion is the dominant mechanism for the oxide formation during the initial stages of oxidation in dry oxygen atmosphere [5–7]. In this work we investigate the effect of oxidation temperature on the oxide growth on Cu(1 1 0) surface during the initial stages of oxidation and the effect of oxygen pressure on the nucleation of oxide islands. The results presented here reveal the differences observed for Cu(1 0 0) and Cu(1 1 0) and the effects of surface structure on the oxidation kinetics, thereby on oxide morphology.

* Corresponding author. Tel.: +1-412-6249753; fax: +1-412-6248016.
E-mail address: guzst1@pitt.edu (G. Zhou).

0169-4332/$ – see front matter
doi:10.1016/j.apsusc.2003.09.008

Copper forms two thermodynamically stable oxides, Cu_2O and CuO. Cu_2O is simple cubic lattice (space group: *pn*3*m*) with 4Cu and 2O atoms in its basis, and a lattice parameter of 4.22 Å. The Cu atoms form a FCC lattice and the O atoms form a bcc lattice, where each O atom is surrounded by a tetrahedron of Cu atoms. CuO has a monoclinic structure. Cu is a FCC metal with a lattice parameter of 3.6 Å. For the temperatures and very low oxygen partial pressures used in our experiments, only Cu_2O is expected to form [8].

2. Experimental

The microscope used in this work was a modified JEOL 200CX [9]. A leak valve attached to the column of the microscope permits the introduction of gases directly into the microscope. In order to minimize the contamination, a UHV chamber was attached to the middle of the column, where the base pressure was less than 10^{-8} Torr without the use of the cryoshroud. The microscope was operated at 100 keV to minimize irradiation effects. Scientific grade oxygen gas of 99.999% purity can be admitted into the column of the microscope through the leak valve at a partial pressure between 5×10^{-5} and 760 Torr. The specially designed sample holder allows for resistive heating at temperatures between room temperature and 1000 °C. Single crystal 99.999% pure 700 Å Cu films were grown on NaCl(1 1 0) substrates in an UHV e-beam evaporation system, then removed from the substrate by dissolving the NaCl in de-ionized water. The Cu film was floated onto a Si piece that is resistively heated in situ. The native Cu oxide was removed inside the TEM by annealing the Cu films in methanol vapor at a pressure of 5×10^{-5} Torr and 350 °C, which reduces the copper oxides to copper [10]. After removal from the in situ TEM investigation, the samples were analyzed using a Digital Instruments NanoScope IIIa scanned probe microscope. Contacting-mode atomic force microscope (AFM) height images were employed to assess the sample surface topology.

3. Results

3.1. Effect of oxidation temperature on oxide growth

We examined the Cu_2O island formation as a function of oxidation temperature in the range of 450–650 °C at 0.1 Torr of oxygen pressure. Three-dimensional island formation was observed for all the temperatures, and the selected area electron diffraction pattern of the Cu_2O island and the underlying Cu(1 1 0) substrate revealed that the oxide island is epitaxial with the Cu substrate, i.e. $(0\,1\,\bar{1})$Cu‖$(0\,1\,\bar{1})Cu_2O$ and (1 0 0)Cu‖(1 0 0)Cu_2O, as shown in Fig. 1.

Fig. 2 shows the dark field TEM images of the oxide islands formed at the different oxidation temperatures

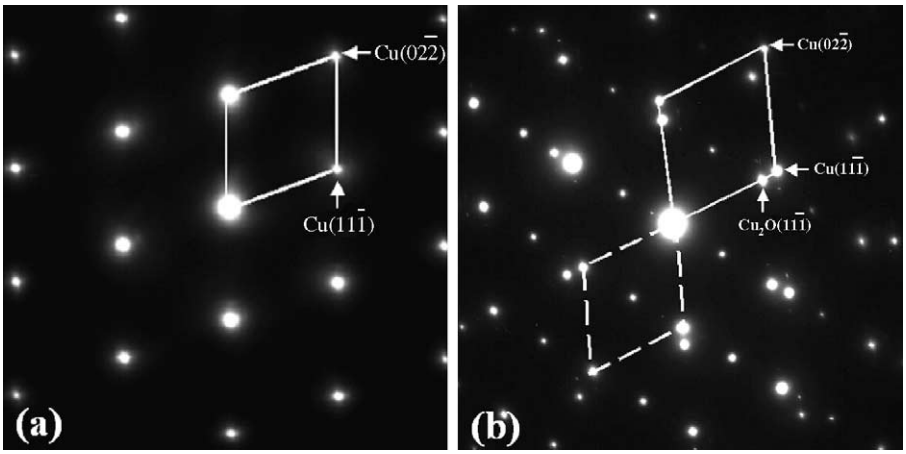

Fig. 1. The epitaxial growth of the oxide on Cu(1 1 0) surface: (a) before oxidation; (b) after oxidation.

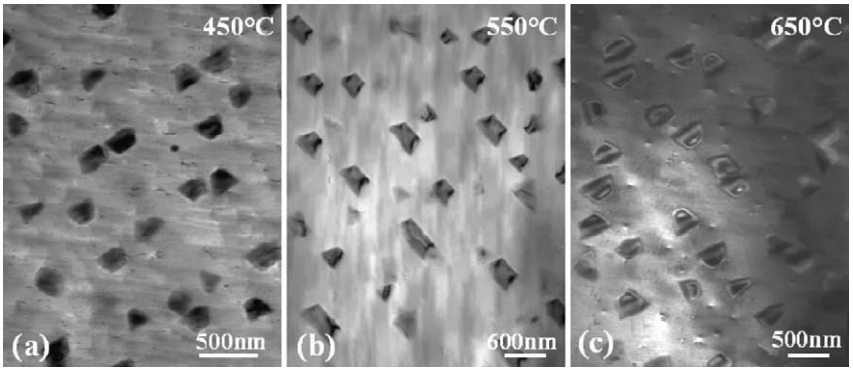

Fig. 2. The dark field images of oxide islands formed on Cu(1 1 0) at the different oxidation temperatures, the oxygen pressure is 0.1 Torr.

but constant oxygen pressure of 0.1 Torr and same oxidation time of 10 min ($\sim 6 \times 10^7$ l), where the Cu(1 1 1) reflection was used for imaging. The oxide islands formed at the different oxidation temperatures have the same trapezoid cross-sectional shape, but different TEM thickness fringe contrast. Fig. 2(a) shows that no thickness fringe contrast occurred in the islands with the lateral size of ~250 nm at the low temperature oxidation (~450 °C). Fig. 2(b) reveals that the oxidation at the elevated temperature (~500 °C) resulted in thickness fringe contrast in the island at the lateral size of ~250 nm. The oxidation at 650 °C caused the sharp thickness fringe contrast in the island at the size of 200 nm.

From the Howie–Whelan equations, the intensity from diffraction beam g is directly proportional to $\sin^2(\pi t/\xi_g)$ in Bragg condition, where t is sample thickness, and ξ_g is the extinction distance. Therefore, the sample thickness can be estimated by the periodicity of the thickness fringe and ξ_g [11]. By applying this relationship, we made a rough estimation of the island thickness. $\xi_{Cu(1\ 1\ 1)}$ is 24 nm for the 100 kV electron beam. In Fig. 2(a), since no thickness fringes occur in the islands, the thickness variation of Cu substrate along Cu/Cu_2O interface is less than 24 nm. In Fig. 2(c), two dark fringes occurred, the thickness variation of the Cu film along the interface is close to 36 nm. The thickness variation of the Cu film in Fig. 2(b) is in the range of 24–36 nm.

Fig. 3(a) shows the AFM image of the Cu_2O islands obtained at 650 °C, which reveals the trapezoid cross-sectional morphology of the island, similar as the TEM observation. Fig. 3(b) shows the cross-sectional profile along the marked line in Fig. 3(a). The surface topology reveals that the oxide island has a flat top and the island height is approximately equal to 23 nm. The island thickness underneath the Cu film was estimated to be ~40 nm by considering the conversion of the displaced copper atoms that had occupied the region of the Cu_2O island. The AFM image analysis of the islands obtained at the lower temperatures revealed the similar features of the islands, i.e., contact angle, island surface flatness, as Fig. 3, but different island heights. The height of the islands formed at 550 °C is ~16 nm, and the island thickness underneath the Cu film was estimated to be ~25 nm, similarly, the penetration thickness of the islands formed at 450 °C was calculated to be ~22 nm. By measuring the contact angles between the island side-facets and the Cu substrate and combining the epitaxial relationship between Cu and Cu_2O (Fig. 3c), we determined the island structural geometry as shown in Fig. 3(d).

3.2. Effect of oxygen pressure on oxide nucleation

One consequence of oxygen surface diffusion being the mechanism for nucleation is that there is a saturation density of oxide islands [12]. This is due to the existence of an active zone of oxygen capture around each oxide island, where the radius of this zone is dependent of oxygen pressure and oxidation temperature. For a constant oxygen pressure, the saturation island density dependence on temperature follows an Arrhenius relationship, $N_s \sim e^{-E_a/kT}$, where k is Boltzmann constant, T is the oxidation temperature, E_a is the activation energy for the oxide nucleation which depends on the energies of nucleation, oxygen surface diffusion, absorption and/or desorption [13].

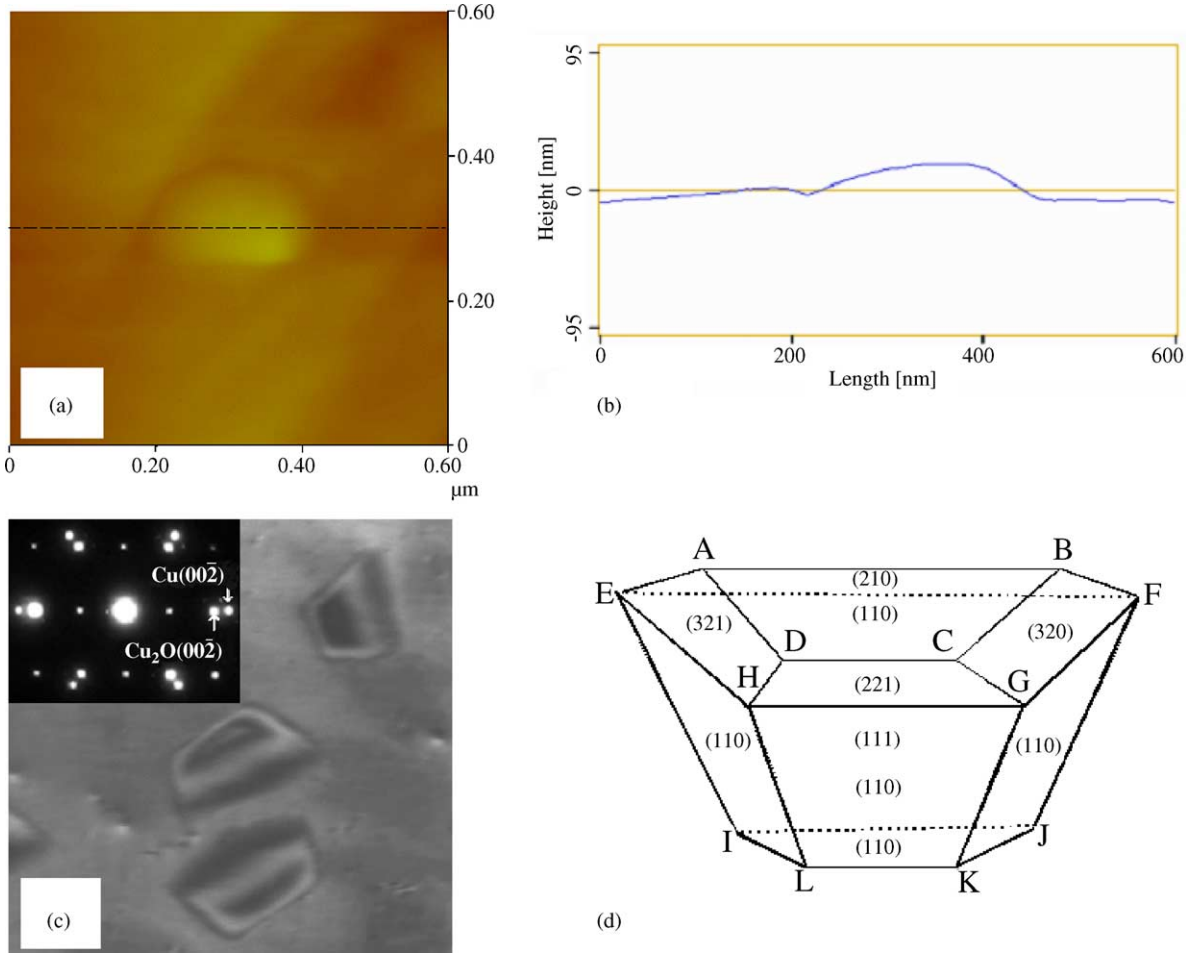

Fig. 3. (a) AFM image of Cu_2O islands formed on Cu(1 1 0) at 650 °C; (b) cross-sectional profile drawn along the marked lines indicated in (a); (c) the epitaxial relationship of the islands with substrate; (d) structure model of the island based on the AFM and TEM measurements.

We measured the saturation density of the oxide islands at the temperatures from 450 to 650 °C at the oxygen pressure. Fig. 4 shows the saturation density of islands versus inverse oxidation temperature. This Arrhenius dependence of the saturation island density on temperature demonstrates the oxygen surface diffusion dominated nucleation processes of the oxide islands. The activation energy, E_a, which is equal to the slope in Fig. 4, was determined to be 0.4 ± 0.04 eV. In comparison, the activation energy, E_a, for Cu(1 1 0) at the temperatures between 300 and 450 °C at constant oxygen pressure of 5×10^{-4} Torr was measured to be 1.1 ± 0.2 eV [7].

The oxygen surface model assumes homogeneous nucleation, not heterogeneous nucleation [12]. One particularly interesting question is the role of surface defects, such as dislocation and steps in the initial stages of oxidation. In the oxidation of Cu(1 0 0), no preferential nucleation sites at dislocations or surface steps were observed [12,14]. Similar as in the oxidation of Cu(1 0 0), repeated oxidation, reduction, followed by oxidation experiments were performed, the new oxide islands were not necessary nucleated at the same positions, and the islands still had a random distribution [15]. Also, the oxide island density was observed to decrease with increasing temperature,

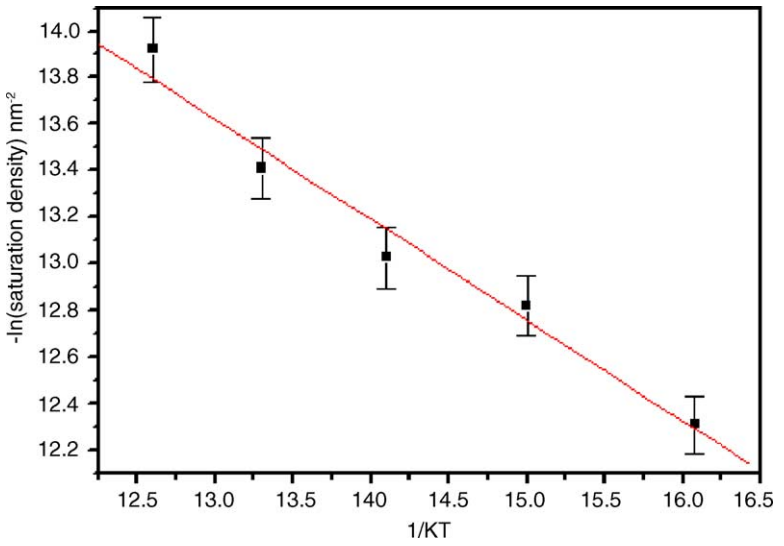

Fig. 4. Cu_2O saturation island density vs. inverse temperature. The absolute value of the slope is the E_a for the surface-limited process.

following as Arrhenius dependence, indicates that nucleation was homogeneous. If the nucleation mechanism was heterogeneous, then it would be reasonable to expect similar island density at different temperatures, which was not observed.

4. Discussion

4.1. Effects of temperature on the kinetics/energetics of oxide formation

During the initial stages of the oxidation, the growth of the oxide islands is accompanied by the conversion of copper atoms to Cu_2O islands along the Cu/Cu_2O edge. Fig. 2 indicates that the oxidation temperature had a large effect on the island thickness growth, i.e., the oxidation at high temperature tends to cause a deep penetration into the Cu substrate. The penetration of the islands into the Cu substrate creates inclined Cu/Cu_2O interface which causes the TEM thickness fringe contrast. Fig. 5 is the schematics of the islands formed at the different temperatures. At the low temperature, 450 °C, the islands have a shallow penetration into the substrate, and a small thickness variation as shown in Fig. 5(a). The oxidation at the high temperature results in formation of the islands with deeper penetration, and a large thickness variation along the inclined interface as shown in Fig. 5(b) and (c).

The oxide island structure is controlled by thermodynamic and/or kinetic factors during the oxidation reaction. The free energy change for the formation of oxide islands can be expressed as

$$\Delta G = \sum A_s\gamma_s + \sum A_i\gamma_i + \Delta G_{vol}(Cu_2O) - \sum A_{Cu}\gamma_{Cu} \quad (1)$$

where $\sum A_s\gamma_s$ is the island surface energy, $\sum A_i\gamma_i$ is the interfacial strain energy, $\Delta G_{vol}(Cu_2O)$ is the volume energy for the formation of Cu_2O, and $\sum A_{Cu}\gamma_{Cu}$ is the surface energy of Cu before the oxide

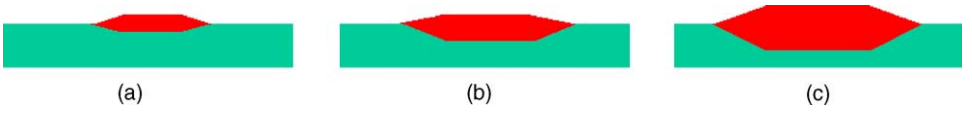

Fig. 5. Schematics of the oxide islands formed at the different oxidation temperatures: (a) 450 °C; (b) 550 °C; (c) 650 °C.

formation. It is known that Cu_2O has a thermal expansion coefficient of $1.9 \times 10^{-6}\ ^{\circ}C^{-1}$, and Cu has a thermal expansion coefficient of $17 \times 10^{-6}\ ^{\circ}C^{-1}$. With temperature increasing, the lattice mismatch (~17%) between Cu and Cu_2O becomes smaller and this lattice mismatch induced interfacial strain is reduced. Therefore, the islands tend to prefer the structure with large interface area which has a deeper penetration at high temperature, such that a thicker oxide island (and more compact) formed at high temperature is more energetically favorable than an island with larger surface area.

We have considered the energetics, but the island growth depends also upon the kinetics. The formation of Cu_2O islands on Cu creates Cu_2O/Cu interface. Their large lattice mismatch causes an interfacial strain field on the Cu/Cu_2O interface. It has been reported that strain fields around islands have an effect on the island growth kinetics in thin film growth processes, i.e., creating additional activation barriers for the incorporation of adatoms to islands [16]. Similarly, in the initial stages of oxidation, the oxide island growth involves the incorporation of oxygen atoms and the strain field concentrated on Cu/Cu_2O interface would inhibit the interface diffusion of oxygen. The oxygen diffusion coefficient D follows an Arrhenius relationship, $D \sim e^{-E_a/kT}$, where E_a is the activation energy for diffusion. Different oxidation mechanisms have different E_a values. It is well known that activation energy for surface diffusion is typically smaller than the other diffusion mechanisms and it has been previously demonstrated the oxide growth is dominated by the surface diffusion of oxygen to the perimeter of the oxide islands when the temperature is lower than 450 °C in the oxidation of Cu(1 1 0) [7]. However, with the oxidation temperature increasing, the Cu and Cu_2O lattice mismatch is reduced and the interface strain is decreased. This reduced strain field near the interface permits diffusion to occur more readily. As a result, there is an enhanced kinetics of oxygen interfacial diffusion which contributes significantly to the thickening growth of the oxide island.

4.2. Effect of oxygen pressure on the activation energy for the oxide nucleation

The initial stages of oxidation proceed through a similar sequence of steps as that typical of condensed vapors to a first approximation. The stages involve oxygen surface adsorption, surface mobility, rearrangements in the adsorbed layer and trapping of the mobile oxygen to form relatively stable and usually ordered structures. On the other hand, rigorous formulation of the nucleation and growth process for oxide formation is more complex than simple vapor condensation. The thermodynamic parameters characteristic to the reaction species are more difficult to evaluate, and the reaction path is more complex. However, it is possible to formulate a simple model which is helpful and to make qualitative predictions from it for experiments where conditions are carefully controlled. In order to form oxide islands on the surface, the system should overcome an activation barrier whose height is given by the work of formation of the critical nuclei. We consider the heterogeneous nucleation of the oxide islands, this activation energy was easily obtained to be

$$\Delta G^* = f(\theta)\sigma^3 \frac{1}{(\Delta G_V + \Delta G_S)^2}, \tag{2}$$

where $f(\theta)$ is the geometric factor of the surface energy, σ the oxide surface energy, ΔG_V the free-energy change which drives the oxidation reaction, and ΔG_S is the strain energy due to the lattice mismatch between the oxide and the metal substrate. ΔG_V can be determined through the oxidation reaction, $2Cu + (\frac{1}{2})O_2 = Cu_2O$

$$\Delta G_V = \Delta G^\circ - \tfrac{1}{2} RT \ln P_{O_2} \tag{3}$$

where R is the gas constant, T the oxidation temperature, P_{O_2} the oxygen pressure, and ΔG° is the standard free change for the formation of Cu_2O and in our oxidation temperature range it is

$$\Delta G^\circ\ (\mathrm{J/mol}) = -130,930 + 94.5T. \tag{4}$$

By applying the above deviation, we consider the effects of the oxygen pressure on the nucleation thermodynamics. Because the sign of ΔG° is negative, ΔG_V will be more negative with the increase in the oxygen pressure. While ΔG_S is positive, the overall energy barrier to nucleation, ΔG^*, decreases with the increase in the oxygen pressure. This analysis is consistent with our measurements that activation energy for the oxide formation at the oxygen pressure of 0.1 Torr is 0.4 ± 0.04 eV, which is smaller than the oxidation at the oxygen pressure of 5×10^{-4} Torr

where the activation energy was measured to be 1.1 ± 0.2 eV [7].

4.3. Comparison to Cu(1 0 0) oxidation

It has been demonstrated that temperature has a dramatic effect on the oxide morphology in the oxidation of Cu(1 0 0) films, and it was found that the oxide morphology can be either triangular shape (~350 °C), square shape (400–550 °C), rod shape (~600 °C) or pyramid shape (650–800 °C) depending only on the oxidation temperature, and the oxide morphology is controlled by kinetics or energetics factors [17,18]. However, in the oxidation of the Cu(1 1 0), the oxidation at the different temperatures (150–650 °C) [7] resulted in the same oxide structure (trapezoid shape). The only difference is that the oxidation at higher temperatures results in the oxide islands with thick penetration into the substrate.

In the oxidation of Cu(1 0 0), no thickness fringe contrast occurred in the TEM observation of the oxide islands with lateral size up to ~650 nm obtained at the different oxidation temperature up to 800 °C [17,18]. Therefore, the oxide islands on Cu(1 0 0) surface show a much more rapid lateral growth rate than the thickening, and the oxide island formation can be considered as a surface process. Consequently, the morphology of the oxide islands can be controlled by the different mechanisms, i.e., surface energetics and/or surface kinetics. The present result indicates that the Cu(1 1 0) surface exhibits a faster thickening growth of the oxide islands than Cu(1 0 0), especially at the high temperature oxidation. It is known that Cu(1 0 0) has a more compact O-chemisorbed surface structure than Cu(1 1 0) surface (corrugated O-chemisorbed structure) [19–22]. It is reasonable to expect that the Cu(1 1 0) surface has a larger activation energy for the oxygen surface diffusion than Cu(1 0 0). This O-chemisorbed roughness on Cu(1 1 0) surface decreases the difference in the activation energies between oxygen surface diffusion and interface diffusion, especially at the high temperature, where the interface diffusion of oxygen is greatly enhanced. Therefore, with temperature increasing, the oxide islands formed on Cu(1 1 0) have a deeper penetration and a more compact structure. It is interesting to expect from the present work that the surface structure has a dramatic effect on the oxide growth mode, and a rough surface will give rise to a fast thickening of oxide islands.

5. Conclusion

Oxidation temperature has a large effect on the kinetics/energetics of the oxide formation, thereby on the oxide structure on Cu(1 1 0) surfaces. With the oxidation temperature increasing, there is a decrease in the lattice mismatch between Cu and Cu_2O due to their different thermal expansion coefficients, and this reduced mismatch causes the enhanced kinetics of oxygen interfacial diffusion which gives rise to the faster oxide thickening rate, especially when the oxidation temperature exceeds 600 °C. The comparison to the lower oxygen pressure oxidation indicates that the oxidation at higher oxygen pressure will result in an easier oxide nucleation. The comparison to the oxidation of Cu(1 0 0) surface indicates that Cu(1 1 0) shows a faster three-dimensional oxide island growth at the elevated oxidation temperature.

Acknowledgements

This research project is funded by National Science Foundation (#9902863) and National Association of Corrosion Engineers (NACE) seed grant. The experiments were performed at the Materials Research Laboratory, University of Illinois at Urbana-Champaign, which is supported by the US Department of Energy (#DEFG02-96-ER45439). The authors kindly thank I. Petrov, R. Twesten, M. Marshall, K. Colravy, and N. Finnegan for their help.

References

[1] J.M. Rakowski, G.H. Meier, F.S. Pettit, F. Dettenwanger, E. Schumann, M. Ruhle, Scripta Mater. 35 (1996) 1417.
[2] F. Young, J. Cathcart, A. Gwathmey, Acta Metall. 4 (1956) 145.
[3] R.H. Milne, A. Howie, Philos. Mag. A 49 (1984) 665.
[4] A. Roennquist, H. Fischmeister, J. Inst. Met. 89 (1960/1961) 65.
[5] J.C. Yang, B. Kolasa, J.M. Gibson, M. Yeadon, Appl. Phys. Lett. 73 (1998) 2481.

[6] J.C. Yang, M. Yeadon, B. Kolasa, J.M. Gibson, Appl. Phys. Lett. 70 (1997) 3522.
[7] G.W. Zhou, J.C. Yang, Surf. Sci. 531–533 (2003) 359.
[8] G. Honjo, Phys. Soc. Jpn. J. 4 (1949) 330.
[9] M.L. McDonald, J.M. Gibson, F.C. Unterwald, Rev. Sci. Instrum. 60 (1989) 700.
[10] S.M. Francis, F.M. Leibsle, S. Haq, N. Xiang, M. Bowker, Surf. Sci. 315 (1994) 284.
[11] P.B. Hirsch, A. Howie, R.B. Nicholson, D.W. Pashley, M.J. Whelan, Electron Microscopy of Thin Crystals, second ed., Krieger, Huntington, New York, 1977.
[12] J.C. Yang, M. Yeadon, B. Kolasa, J.M. Gibson, Scripta Mater. 38 (1998) 1237.
[13] J.A. Venables, G.D.T. Spiller, M. Hanbuecken, Rep. Prog. Phys. 47 (1984) 399.
[14] J.C. Yang, M. Yeadon, B. Kolasa, J.M. Gibson, J. Electrochem. Soc. 146 (1999) 2103.
[15] G.W. Zhou, J.C. Yang, in preparation.
[16] E. Penev, P. Kratzer, M. Scheffler, Phys. Rev. B 8 (2001) 5401.
[17] G.W. Zhou, J.C. Yang, Appl. Surf. Sci. 210 (3–4) (2003) 165.
[18] G.W. Zhou, J.C. Yang, Phys. Rev. Lett. 89 (2002) 106101.
[19] J.G. Tobin, L.E. Klebanoff, D.H. Rosenblatt, R.F. Davis, Phys. Rev. B 26 (1982) 7076.
[20] K.W. Jacobsen, J.K. Nørskov, Phys. Rev. Lett. 65 (1990) 1788.
[21] F. Jensen, F. Besenbacher, E. Lægsgaard, I. Stensgaard, Phys. Rev. B 42 (1990) 9206.
[22] I.K. Robinson, E. Vlieg, Phys. Rev. B 42 (1990) 6954.